

Influence of Human Limb Motion Speed in a Collaborative Hand-over Task

Matteo Melchiorre, Leonardo Sabatino Scimmi, Stefano Mauro and Stefano Pastorelli

Department of Mechanical and Aerospace Engineering, Politecnico di Torino, C.so Duca degli Abruzzi 24, Turin, Italy

Keywords: Collaborative Robotics, Human Robot Hand Over, Trajectory Planning, Motion Tracking.

Abstract: The paper analyses a possible cooperative task between a human operator and a robot. Operator and robot are interfaced by Microsoft Kinect® which is used to detect the position of an upper limb of the operator. The robot is driven by a control algorithm designed to track the hand of the human and to obtain a hand-over in the final part of the trajectory. The paper describes the algorithm and shows its performance with different velocities of the limbs by means of tests carried out in a simulation environment.

1 INTRODUCTION

The most recent manufacturing scenario is moving towards the integration of robot's and human's workspace in which the cooperation assumes a central role and defines a specific field of research for human-assistance application. Thus, the most fascinating challenge is to safely approach the machines to the human, especially in the industrial context, in order to reduce the risk of injuries and the completion of repetitive tasks, respectively lightening the workers fatigue and stress. Moreover, the introduction of collaborative robots (cobots) in the workstations is synonymous of flexibility and changeability. All the mentioned advantages clearly represent a potential increase in terms of productivity.

There are many works contributing to fully focus the state of the art in Human Robot Collaboration (HRC). Bo et al. (2016) present a brief description of the classical robotics industrial application, while a more detailed overview on HRC is given by Kruger et al. (2009). The latter identifies an interesting classification of cooperative systems, distinguishing the "workplace sharing systems" from "workplace and time sharing systems". In the "workplace sharing systems" human and robot perform separated task within a shared environment and the interaction between them is limited to collision avoidance; the "workplace and time sharing systems" indicates the possibility to jointly handle objects in a level much deeper than just the avoidance of collision. This work stands in the second type of systems and it is focused

on the study of human-robot interaction (HRI) in handing-over applications, describing the results obtained in the development of an algorithm to drive the end effector of the robot towards the human hand while carrying out a collaborative task.

In literature there are several works introducing HRI in industrial environments. Michalos et al (2014) describe a case study whose final level is the execution of the same assembly task by the robot and the human being in direct physical interaction; Cherubini et al (2016) propose a full and concrete example of an assembly application in which a LBR iiwa is controlled in real time using a RGB camera and admittance control in order to execute the task safely with the human operator. Zahe and Roesel (2009) also discuss an assembly process, performed by human and robot, monitored by various sensors. All the cited examples move towards the industrial application, thus suffers the very restrictive safety constraints which close to a complete integration of human and robot: tasks are carried out sequentially and there is not cooperation at the level of hand-over the objects to be assembled.

Other works studies the HRI without strictly referring to industrial application. They are useful to understand the closer relationship between humans' behaviour and robot's capability while assisting them. Agah and Tanie (1997) investigate the problem of a human receiving object from a mobile manipulator, which is controlled through an algorithm based on fuzzy logic, simulating a simple 2D model of both human limb and robotic 3DOFs arm. Huber et al (2008) describe the interaction of human and robot in

a handing-over task, driving the manipulator along fixed trajectories and discussing the influence of the robot velocities in people perception. A similar study is proposed in (Shibata et al, 1997), where the relationship between the human-human and human-robot hand-over is analysed, also considering the influence of the final hand-over position of the robot end effector and the human hand.

This work aims to contextualize the hand-over task in a collaborative environment, investigating the behaviour of a cobot following the human operator hand, which is tracked by means of a multi-vision system. Additionally, in order to integrate the hand-over with the cooperative task, the collision avoidance will be also considered to evaluate the total computation time for a complete collaborative algorithm (Mauro et al., 2017), (Mauro et al., 2018).

The collaborative space consists of a working table over which it is placed a collaborative robot; a man is standing in front of the robot and he is supposed to hand-over a component in different positions on the table. The trajectory of the hand of the human is detected by two Microsoft Kinect®, and the measured signal is used to update the trajectory of the robot. Tests are carried out in a simulated environment including a kinematic model of the Kuka LBR iiwa R820 robot, which is interfaced with actual signal experimentally measured. The results show the trajectory followed by the robot in several tests, considering different limb velocities and different final positions for the hand of the operator.

The paper is structured as follow: in section 2 the layout of the shared workspace is presented, introducing the task and the elements which characterize the collaborative space. Section 3 describes the hand-following algorithm together with the simulation tools; the experimental setup and the method for spatial synchronization are described in section 4. Finally, section 5 discusses the main results of the experiments.

2 THE COLLABORATIVE TASK

The collaborative operation is carried out in a workspace which is shared between the human operator and the robot. The task is performed on a working table and the human operator is standing in front of it, along one of its long sides. The robot is installed at the opposite side of the table, as shown in Figure 1.

Two Microsoft Kinect® are displaced on the same side of the robot and detect the motion of the upper limbs of the human operator. The use of two sensors

allows to prevent full occlusion cases, since the robot could represent an obstacle for human tracking while executing the task. In order to ensure the correct positioning of the points detected by the motion capture system, 3 reference points are displaced in the workspace and are used to build the reference frame \mathcal{F}_R when the system is initialised.

The robot is only virtual and human-robot interaction is simulated in Matlab by interfacing the experimental data measured by the motion capture system with a model of the robot, which is operating in the same virtual workspace.

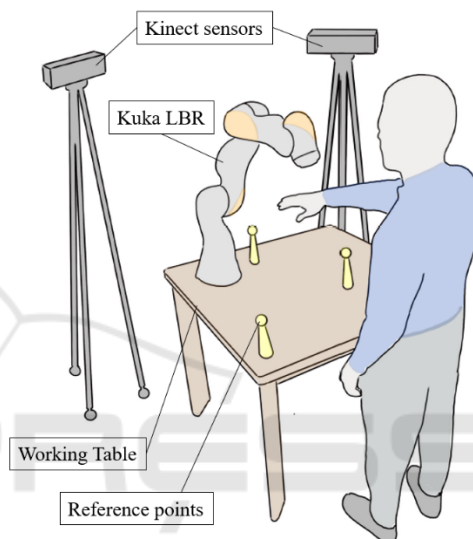


Figure 1: Shared workspace.

The performed task consists in making possible a hand-over between the hand of the man and the end-effector of the robot. The robot is driven in order to track with its end effector the position of the hand of the human operator until these two parts come in contact.

The tests are carried out considering the case in which the man extends its right upper limb to reach a hand-over area on the workbench. According to the position detected by the motion tracking system, the robot reacts and drives its end effector towards the final position reached by the hand of the operator.

In order to study a potentially collaborative task, the hand-over can happen in four different portions of the working space, identified as meeting volumes V_{MP} , which are represented in Figure 2. These volumes are shaped as four spheres centred in the ideal meeting points **MPs** and are chosen so that they almost entirely cover the volume reachable by the human with his extended arm, standing beside the workbench.

Five different velocities are considered for the motion of the human limb. However, as the trajectories should certainly change if an operator performed the same motion with different velocities, only one movement towards each of the MPs was acquired. The time history of the position of the human skeleton joints identified by the Kinect sensor was then modulated by scaling the total time T times 0.6, 0.8, 1.3 and 1.6. Thus, slower and faster motions were simulated. Finally, the signal was interpolated and resampled to consider the effect of the Kinect refresh time. The sampling frequency was assumed to be 30 Hz, as provided by datasheet and verified during experimental tests.

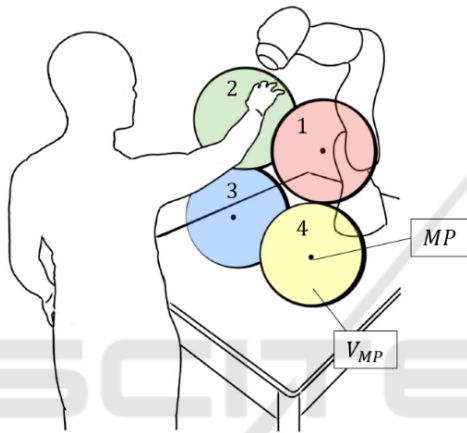


Figure 2: Meeting points and their V_{MP} volumes.

3 HAND-FOLLOWING ALGORITHM

3.1 Motion Planning

The problem of observing and following a moving target has already been studied in different applications. Houshangi (1990) gave interesting results on grasping a moving object with a 6DOF manipulator using vision. In this section the method of motion planning based on separation of the direction and size of velocity in the working space is adopted, using the inverse kinematics algorithm and a principle similar to (Bing & Xiang, 2008), (Dong & Zhu, 2016).

The available data from the sensors is the position of the human hand \mathbf{p}_h measured with a sampling time Δt_k . The position \mathbf{p}_e and orientation ϕ_e of the end-effector are also known from forward kinematic. Starting from this information, the operational space

error \mathbf{e}_k between the desired and actual end-effector position at sample k , can be written using the generalized vectors $\mathbf{x}_{e,k}$ and $\mathbf{x}_{h,k}$ as

$$\mathbf{e}_k = \mathbf{x}_{h,k} - \mathbf{x}_{e,k} = \begin{bmatrix} \mathbf{e}_{p,k} \\ \mathbf{e}_{\phi,k} \end{bmatrix} \quad (1)$$

$$\mathbf{x}_{e,k} = \begin{bmatrix} \mathbf{p}_{e,k} \\ \phi_{e,k} \end{bmatrix} \quad \mathbf{x}_{h,k} = \begin{bmatrix} \mathbf{p}_{h,k} \\ \phi_{h,k} \end{bmatrix} \quad (2)$$

where $\phi_{h,k}$ is the end-effector desired final orientation, which in each test is assumed to be equal to the initial value. To drive the end-effector towards the target, intuitively its linear velocity is set as:

$$\dot{\mathbf{p}}_{e,k} = C \mathbf{e}_{p,k} = C e_{p,k} \hat{\mathbf{h}}_k \quad (3)$$

with a direction $\hat{\mathbf{h}}_k$ pointing the target and a magnitude proportional to the position error through the constant C depending on the application (Figure 3). The same approach is used to define the angular velocity, which is modelled proportional to the orientation error written in terms of unit quaternion $\mathbf{e}_{o,k}$ (Siciliano et al, 2009). The generalized velocity vector of the end-effector becomes:

$$\mathbf{v}_{e,k} = C \begin{bmatrix} \mathbf{e}_{p,k} \\ \mathbf{e}_{o,k} \end{bmatrix} \quad (4)$$

Thus, the joint velocity vector at time k is obtained by inverting the Jacobian:

$$\dot{\mathbf{q}}_k = J_k^{-1} C \begin{bmatrix} \mathbf{e}_{p,k} \\ \mathbf{e}_{o,k} \end{bmatrix} \quad (5)$$

At the end, joints position is computed by means of first order integration. The dynamic behaviour of the robot was also considered by modelling the velocity response of each servo axis as a first order system.

For the purpose of this paper, it is reasonable to limit the maximum value of the linear velocity of the end-effector to 0.25 ms^{-1} . This choice is justified by the desire to study a collaborative task (ISO10218-1:2011 "Safety requirements for industrial robots") meeting the requirements for a good hand-over (Jindai et al, 2006). Moreover, a safety margin is introduced to let the end-effector stop at a distance R_H from the human hand (Figure 3).

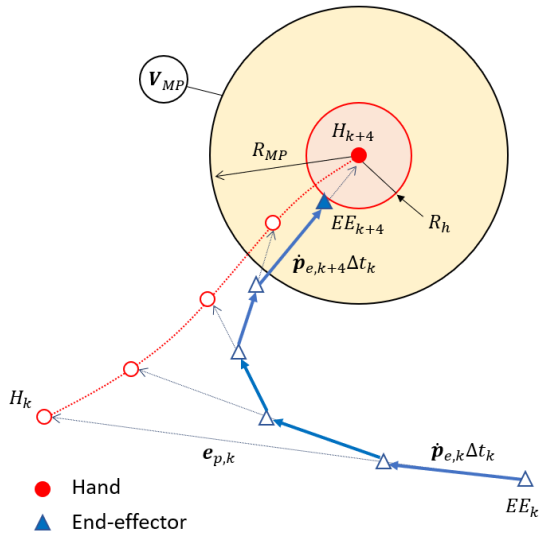


Figure 3: Schematics of the motion planning.

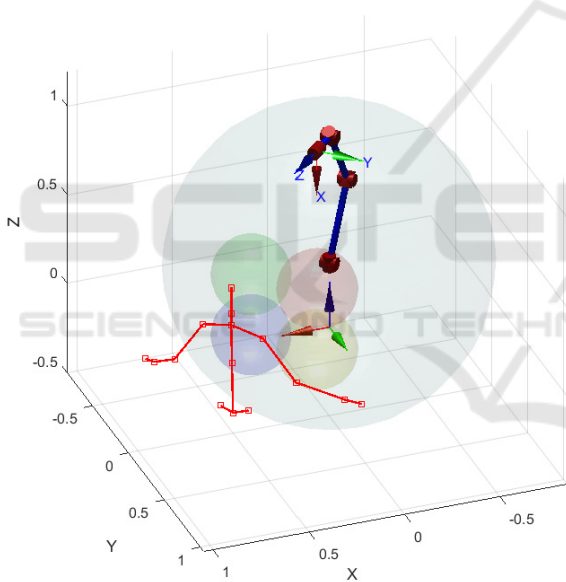


Figure 4: Matlab simulation environment.

3.2 Algorithm and Simulation Tools

The simulation algorithm must implement the motion planning while processing the skeleton data coming from the two Kinect sensors. Moreover, to analyse the total time required for computation in a collaborative environment, the effect of a collision avoidance based on potential fields is added to (4) as described in the work of Mauro et al. (2018).

The interaction of robot with the human is simulated in Matlab. Figure 4 shows the kinematic model of the robot built using the Robotics Toolbox

(Corke, 2017) in its initial pose. In the same figure are also plotted the stick diagram of the human upper body, the operational space of the robot V_{OS} (grey transparent sphere), the four meeting volumes introduced in Figure 2, the reference frame \mathcal{F}_R (at the base of the robot) and the end-effector frame \mathcal{F}_e .

Table 1 schematize the algorithm: once the skeleton $\mathcal{S}_{A,k}$ and $\mathcal{S}_{B,k}$ at sample time t_k are available from both sensors A and B, an optimization is carried out to refine the signal with the duplex Kinect approach (Yeung, Kwok & Wang, 2013); then the initial configuration from the LBR kinematic model is obtained and the hand-following starts only if the human hand results in the operational space of the robot V_{OS} . If the latter condition is met, the following avoiding velocities, $\dot{\mathbf{p}}_{ef,k}$ and $\dot{\mathbf{p}}_{ea,k}$ respectively, are computed to finally obtain the new robot configuration \mathbf{q}_k through inverse kinematics. The robot stops to point toward the target if both the hand of the human and the end-effector meet in one of the ideal meeting point ranges V_{MP} , represented by means of four spheres. Notice that the hand-over can happen in any point inside the coloured spheres.

The specifications of the iiwa R820, obtained from the data sheet of the KUKA LBR, are included in the model. Thus, calculations are made considering the joints angle limits and their velocity range. The joint velocity outputs from the hand-following algorithm are integrated, updating the robot configuration until a new human hand configuration is processed, it means with the Kinect sampling rate $\Delta t_k = 1/30$ s.

Table 1: Algorithm structure.

1. *for* $k \in \{\text{kinect samples}\}$
2. $\mathcal{S}_{A,k}, \mathcal{S}_{B,k}$
3. $\mathcal{S}_{opt,k} \rightarrow \mathbf{p}_{h,k}$
4. $LBR \rightarrow \mathbf{q}_k, \mathbf{J}_k, \mathbf{p}_{e,k}$
5. *if* $\mathbf{p}_{h,k} \in V_{OS} \ \&\& \ \mathbf{p}_{e,k}, \mathbf{p}_{h,k} \notin V_{MP}$
6. *Hand following* $\rightarrow \dot{\mathbf{p}}_{ef,k}$
7. *Collision Avoidance* $\rightarrow \dot{\mathbf{p}}_{ea,k}$
8. $\dot{\mathbf{p}}_{e,k} = \dot{\mathbf{p}}_{ef,k} + \dot{\mathbf{p}}_{ea,k} \rightarrow \mathbf{v}_{e,k}$
9. $\dot{\mathbf{q}}_k = \mathbf{J}_k^{-1} \mathbf{v}_{e,k}$
10. $\mathbf{q}_k = \mathbf{q}_k + \dot{\mathbf{q}}_k \Delta t_k$
11. $\mathbf{q}_{LBR} = \mathbf{q}_k$
12. *else Hand following = false*
13. *end*
14. *end*

4 EXPERIMENTAL TESTING

4.1 Spatial Matching

The multiple sensor approach, combined with the need for simulating the presence of the manipulator, requires that the two operators of the collaborative task, i.e. human and robot, are correctly identified in a common reference frame \mathcal{F}_R . The \mathcal{F}_R must be physical and opportunely built, positioned and oriented in the shared volume so that it can be easily recognized by the two sensors and the human.

The Kinect allows to measure spatial coordinate of objects within its field of view (FOV) in terms of point cloud. Watching this principle and by considering the depth camera resolution, we designed three suitable solid references, characterized by a narrow-conical support with a spherical protruding tip of a 10 mm radius. It was observed that it is easy to distinguish the spherical references in the point cloud to locate them in the Kinect frame (Figure 5-6).

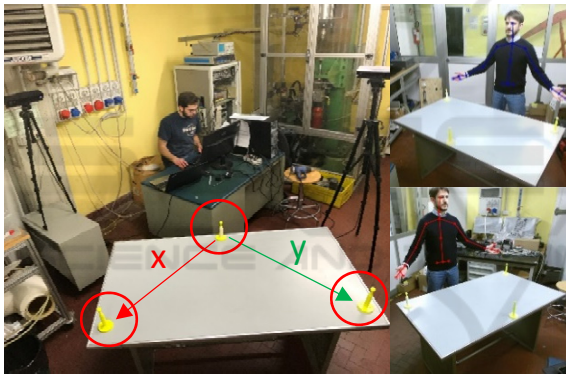


Figure 5: Lab set-up for spatial matching.

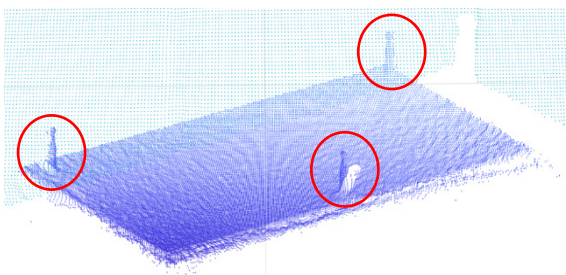


Figure 6: References in the Kinect point cloud.

Figure 5 shows the \mathcal{F}_R placed on the table that represents the workbench. Although the absence of the physical robot might seem a limiting factor, if the coordinates of the base of the manipulator with respect to the \mathcal{F}_R is conveniently defined, it is easy to arrange the meeting points (MPs) as a subset of the

LBR operational space. In this case we assume the base of the robot coincident with the \mathcal{F}_R so that the MPs fill the working volume between the two operators (Figure 7).

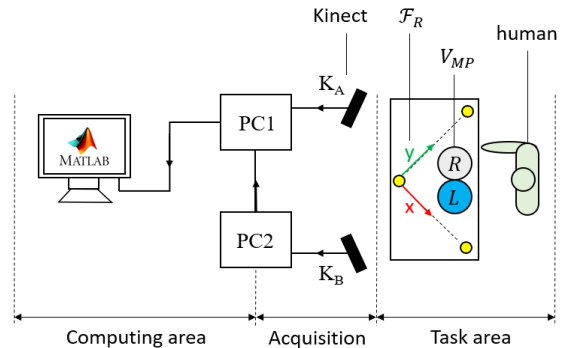


Figure 7: Scheme of the experimental hardware.

4.2 Experimental Set-up

In Figure 7 the schematics of the experimental tools and hardware are presented. The test area can be divided in three main groups which communicate to produce, acquire and process data. The human operator is standing in front of the table, opposite the \mathcal{F}_R origin in which is located the robot, defining the task area. The measurements are performed by the two Kinect sensors, whose FOVs cover the entire volume defined by the task area. Finally, the hardware for data processing is placed outside the views of the depth cameras.

Microsoft Kinect SDK support only one sensor at a time, thus we used two computers to acquire the skeleton data. The PCs are wired so they can send and receive signals each other. In particular, PC1 is designated to handle the start/stop acquisition triggers for the sensors to make the sampling synchronous. Moreover, it collects the raw points from Kinect A and B, executing the algorithms for skeleton optimization and target pursuit. For this purpose, we use two computers with i7-6700 processor and 32 GB RAM.

To inspect the human-robot interaction in different conditions, the tests are conducted at different MPs and velocities of the human hand. This is a powerful approach because it encloses the characteristics of a collaborative task. Thus, the study of different MPs, also taking into account the speed factor, will give information on the behaviour of the operators who are completing the heterogeneous task.

In the experiments the human identifies the MPs by observing two references on the workbench that indicates the projections of the meeting volumes (Figure 7), the latter being inside the operational

space of the robot as mentioned in the previous section. Said projections are named L (left) and R (right). If the shoulders and the hips are then assumed as reference for the z coordinate of the MPs, the meeting volumes V_{MP} are completely defined. The frames in Figure 8 illustrate the four movements corresponding to the various MPs.

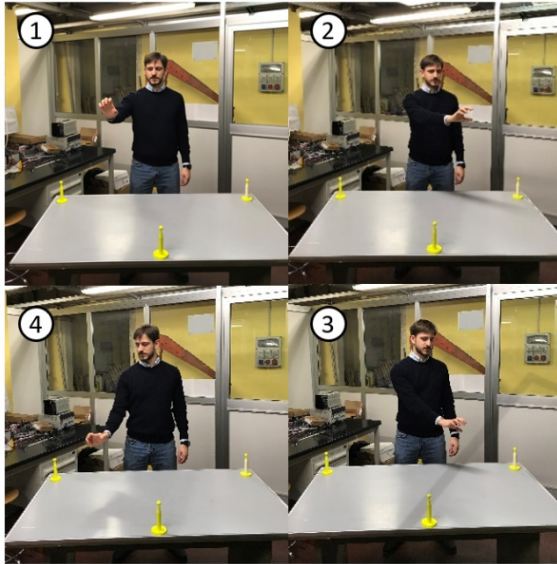


Figure 8: Tested movements of the human hand. The round labels identify the number assigned to each test.

5 RESULTS

Table 2 summarises the simulation parameters used to generate the data presented in this section, while Figure 9 contains the main results of this work.

Figure 9 (a) shows the simulation frames of test 1 with the original values of the hand velocity. In the first frame (left) the hand starts moving and the robot doesn't react because the target is outside its operational space; when the hand is inside the grey volume (second and third frames) the algorithm animates the robot. Finally, the end-effector meets the hand in the meeting volume to accomplish the hand-over task.

To better understand the hand-over time behaviour, Figure 9 (b) illustrates the distance between the end-effector and the human hand versus the original times of tests 1 and 3. If the hand-over happens within the volume of test 1, it can be observed that the hand waits less than a second until seeing the robot entering in the V_{MP} . In test 3 there's a more significant delay due to the different V_{MP} position since the end-effector linear velocity is

limited to 0.25 ms^{-1} for this collaborative task. Notice also that the hand-over happens in all cases at the distance $R_H = 0.1 \text{ m}$.

To analyse the human limb velocity effect on the hand-over sequence, in Figure 9 (c) the time is normalized over the period T , which represents the hand motion total time. For test 1, focusing on the interval within the two operators stop, the red curves show different delays in terms of percentage. For example, the $0.6T$ test shows the human waiting more than $2.5T$ until the robot reaches the meeting point. Furthermore, with a $1.6T$ movement, the hand and the robot would access the meeting volume at almost similar times, representing an interesting scenario. The blue curves of test 3 reveals also different behaviours as function of the velocities. Here the delay goes from $1.7T$ to almost $4T$, the latter representing the worst case. Therefore, the higher the human limb velocity to reach the meeting point, the longer is the task-cycle to accomplish hand-over.

In Figure 9 (e) the hand-over positions for each test, from the point of view of the human operator, are presented. Finally, Figure 9 (d), shows the path of the end-effector and the hand for each test and for different velocities of the human limb. The results show that the robot paths are very close even varying the period T , which is the time the hand needs to reach the meeting points and to stop. In particular, the robot trajectories of test 4 almost coincide, while test 3 is the most susceptible. Thus, in the defined task, the human velocity does not noticeably influence the end-effector trajectories and, most important, the hand-over final relative position of the hand and the robot does not change.

Table 2: Simulation parameters and times.

<i>Collaborative space parameters</i>	
$R_{OS} = 820 \text{ mm}$	
$R_{MP} = 200 \text{ mm}$	
$R_H = 100 \text{ mm}$	
<i>Simulation parameters</i>	
$\mathbf{q}_{k=0} = [\pi/4, -\pi/6, 0, -\pi/3, 0, \pi/3, 0]$	
$C = 10$	
$v_{elin,max} = 0.25 \text{ ms}^{-1}$	
<i>Processing times</i>	
<i>Duplex Kinect alg.</i> = 5 ms	
<i>Collision Avoidance alg.</i> = 10 ms	
<i>Hand Following alg.</i> < 1 ms	

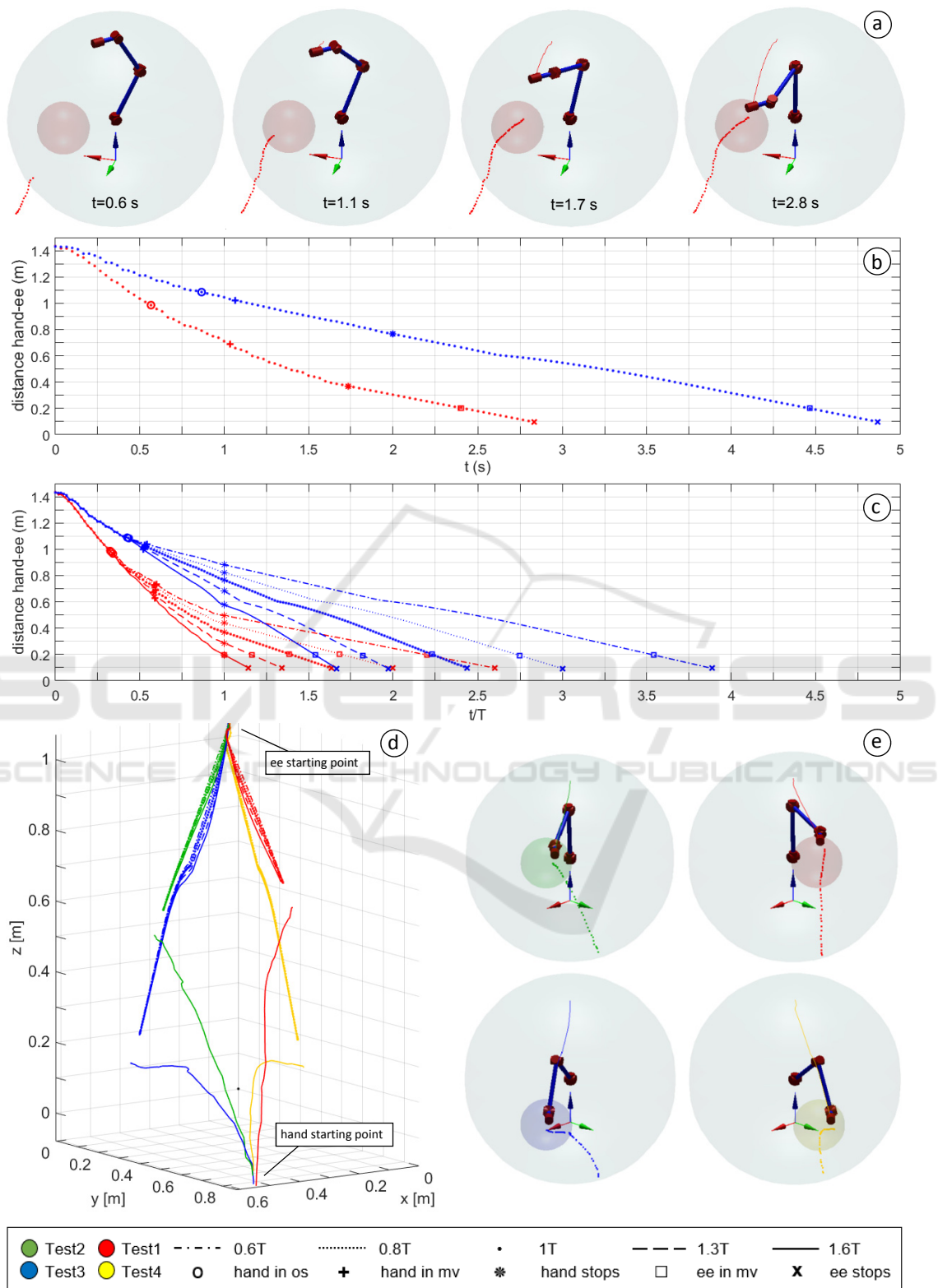


Figure 9: a) Test 1 simulation frames; b) distance hand-ee with original sampling time in test 1 and 3; c) distance hand-ee with normalized time for different values of human limb velocity in test 1 and 3; d) paths of the hand and the ee in the four tests; e) hand-over frames.

6 CONCLUSIONS

In this paper an algorithm, useful for a potentially cooperative task between a human and a robot, is presented. The work contains all the elements which characterize a collaborative space and focuses on the hand-over without restricting the robot to walk predefined paths: the algorithm controls the cobot to permit to the end-effector to reach the hand of the human operator in any point of a dedicated exchanging area.

Experimental tests have been performed to validate the methodology. In these tests, the human hand moves towards four distinct positions with different velocities. Different total times of human limb motion towards the meeting points do not affect the robot paths, but they influence the delay in the hand-over task.

Future works will involve different modelling of the end-effector linear velocity to move the robot with a human-like profile, for example pursuing a minimum-jerk profile or a simple ball-shaped one (Flash et al., 1985). The prediction of the human movements, not considered in this work, will be another important point to refine the algorithm.

REFERENCES

<https://www.iso.org/standard/51330.html>

- Agah, A., and Tanie, K., 1997. Human Interaction with a Service Robot: Mobile-Manipulator Handing Over an Object to a Human. In *Proceedings of the 1997 IEEE International Conference on Robotics and Automation*, New Mexico.
- Bing, W., and Xiang, L., 2008. A Simulation Research on 3D Visual Servoing Robot Tracking and Grasping a Moving Object. In *15th International Conference on Mechatronics and Machine Vision in Practice*, pp. 362-367.
- Bo, H., Mohan, D. M., and Azhar, M., 2016. Human Robot Collaboration for Tooling Path Guidance. In *IEEE International Conference on Biomedical Robotics and Biomechanics*, pp. 1340-1345.
- Cherubini, A., et al, 2016. Collaborative manufacturing with physical human-robot interaction. In *Robotics and Computer-Integrated Manufacturing*, 40, pp. 1-13.
- Corke, P. I., 2017. *Robotics, Vision & Control: Fundamental Algorithms in Matlab*, Springer. London, 2nd edition.
- Dong, G., and Zhu, Z. H., 2016. Incremental visual servo control of robotic manipulator for autonomous capture of non-cooperative target. In *Advanced Robotics*, 30:22, pp. 1458-1465.
- Flash, T., and Hogan, N., 1985. The Coordination of Arm Movements: An Experimentally Confirmed Mathematical Model. In *The Journal of Neuroscience*, 5(7), pp. 1688-1703.
- Houshangi, N., 1990. Control of a robotic manipulator to grasp a moving target using vision. In *Proceedings., IEEE International Conference on Robotics and Automation*, pp. 604-609.
- Huber, M., et al., 2008. Human-Robot Interaction in Handing-Over Tasks. In *Proceedings of the 17th IEEE International Symposium on Robot and Human Interactive Communication*, pp. 107-112.
- Jindai, M., Shibata, S., Yamamoto, T., and Watanabe, T., 2006. A Study on Robot-Human System with Consideration of Individual Preferences. In *JSME International Journal Series C Mechanical Systems, Machine Elements and Manufacturing*, 49, pp. 1033-1039.
- Kruger, J., Lien, T. K., and Verl, A., 2009. Cooperation of human and machines in assembly lines. In *CIRP Annals, Manufacturing Technology*, 58, pp. 628-646.
- Mauro, S., Pastorelli, S., and Scimmi, L.S., 2017. Collision Avoidance Algorithm for Collaborative Robotics. In *Int. J. of Automation Technology*, 11(3):481-489.
- Mauro, S., Scimmi, L. S., and Pastorelli, S., 2018. Collision Avoidance System for Collaborative Robotics. In *Mechanisms and Machine Science*, 49:344:352.
- Michalos, G., et al., 2014. ROBO-PARTNER: Seamless Human-Robot Cooperation for Intelligent, Flexible and Safe Operations in the Assembly Factories of the Future. In *Procedia CIRP*, 23, pp. 71-76.
- Shibata, S., Sahbi, B. M., Tanaka, K., and Shimizu, A., 1997. An Analysis of The Process of Handing Over An Object and Its Application to Robot Motions. In *IEEE International Conference on Systems, Man, and Cybernetics*.
- Siciliano, B., Sciavicco, L., Villani, L., and Oriolo, G., 2009. *Robotics: Modelling, Planning and Control*, Springer. London.
- Yeung, K. Y., Kwok, T.H., and Wang, C. L., 2013. Improved Skeleton Tracking by Duplex Kinects: A Practical Approach for Real-Time Applications. In *Journal of Computing and Information Science in Engineering*, 13(4).
- Zaeh, M., and Roesel, W., 2009. Safety Aspects in a Human-Robot Interaction Scenario: A Human Worker Is Co-operating with an Industrial Robot. In *FIRA 2009: Progress in Robotics*, pp. 53-62.